

Received 19 February 2024; revised 29 May 2024; accepted 2 July 2024.
Date of publication 16 July 2024; date of current version 29 July 2024.

Digital Object Identifier 10.1109/JTEHM.2024.3429422

Variable Stiffness and Damping Mechanism for CPR Manikin to Simulate Mechanical Properties of Human Chest

HYUNGSOO LIM^{1,2}, (Graduate Student Member, IEEE), DONG AH SHIN^{1,3}, (Member, IEEE),
JAEHOON SIM⁴, JAEHEUNG PARK^{1,4,5}, (Member, IEEE), TAEGYUN KIM^{6,7}, KYUNG SU KIM^{6,7},
GIL JOON SUH^{1,6,7,8}, AND JUNG CHAN LEE^{1,9}, (Member, IEEE)

¹Interdisciplinary Program in Bioengineering, Seoul National University Graduate School, Seoul 08826, South Korea

²Integrated Major in Innovative Medical Science, Seoul National University Graduate School, Seoul 08826, South Korea

³Institute of Medical and Biological Engineering, Medical Research Center, Seoul National University, Seoul 08826, South Korea

⁴Graduate School of Convergence Science and Technology, Seoul National University, Seoul 08826, South Korea

⁵Advanced Institute of Convergence Technology (AICT), Suwon-si 16229, South Korea

⁶Research Center for Disaster Medicine, Seoul National University Medical Research Center, Seoul 03080, South Korea

⁷Department of Emergency Medicine, Seoul National University Hospital, Seoul 03080, Republic of Korea

⁸Department of Emergency Medicine, Seoul National University College of Medicine, Seoul 03080, South Korea

⁹Department of Biomedical Engineering, Seoul National University College of Medicine, Seoul 03080, South Korea

(Hyungsoo Lim and Dong Ah Shin are co-first authors.) CORRESPONDING AUTHOR: J. C. LEE (jch@snu.ac.kr)

This work was supported in part by the Basic Science Program through the National Research Foundation of Korea (NRF) funded by the Ministry of Education under Grant 2021R1A6A3A01087371 and in part by Korea Medical Device Development Fund Grants funded by Korea Government under Project RS-2022-00141157.

ABSTRACT Objective: This study introduces a novel system that can simulate diverse mechanical properties of the human chest to enhance the experience of CPR training by reflecting realistic chest conditions of patients. Methods: The proposed system consists of Variable stiffness mechanisms (VSMs) and Variable damper (VD) utilizing stretching silicone bands and dashpot dampers with controllable valves to modulate stiffness and damping, respectively. Cyclic loading was applied with a robot manipulator to the system. Compression force and displacement were measured and analyzed to evaluate the system's mechanical response. Long-term stability of the system was also validated. Results: A non-linear response of the human chest under compression is realized through this design. Test results indicated non-linear force-displacement curves with hysteresis, similar to those observed in the chest of patients. Controlling the VSM and VD allowed for intentional changes in the slope and area of curves that are related to stiffness and damping, respectively. Stiffness and damping of the system were computed using performance test results. The stiffness ranged from 5.34 N/mm to 13.59 N/mm and the damping ranges from 0.127 N·s/mm to 0.511 N·s/mm. These properties cover a significant portion of the reported mechanical properties of the human chests. The system demonstrated satisfactory stability even when it was subjected to maximum stiffness conditions of the long-term compression test. Conclusion: The system is capable of emulating the mechanical properties and behavior of the human chests, thereby enhancing the CPR training experience.

INDEX TERMS Cardiopulmonary resuscitation (CPR), manikin, variable damping, variable stiffness, thorax.

Clinical and Impact: By achieving non-linear mechanical properties including hysteresis, our system has the potential to be used in medical trainings and research studies that reflect more realistic CPR conditions.

I. INTRODUCTION

CARDIOPULMONARY Resuscitation (CPR) is a treatment performed for individuals who have suffered cardiac arrest to restore blood circulation through chest compressions preventing damage to major organs such as

brain, and helping the return of spontaneous circulation (ROSC) [1]. Chest compression is especially related to survival of patients [2], [3]. American Heart Association (AHA) recommends to keep compression depth of 5 cm and compressions speed of 100 to 120 for a minute during CPR [1].

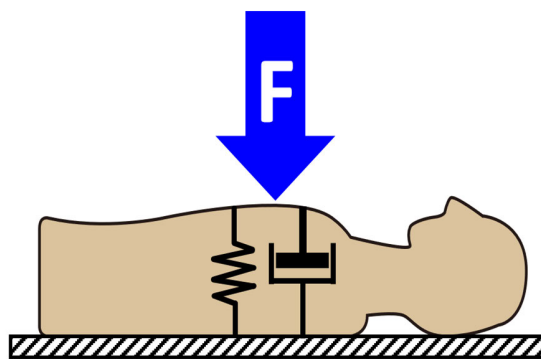


FIGURE 1. Schematic of human chest expressed with mechanical components.

Since compression rates [4] and depth [5] affect the survival rate of the patients [6], it is important to get the technique right. CPR education for resuscitation skill training is usually conducted using manikins that resemble torso of human including silicone skin, a pushing element that acts like a sternum and a spring that exerts stiffness against compression loading. Because of this structure, the manikin shows almost linear behavior on dynamic loading. However, mechanical characteristic of a real human chest demonstrates a non-linear mechanical behavior which can be expressed with not only spring but also damper under dynamic loadings [7], [8], [9] as shown in Fig. 1. Such non-linear mechanical properties may vary by age, gender, and weight [10], [11], [12], [13], [14]. These properties are also affected by changes in CPR conditions such as compression force, depth, and length of time CPR has been performed [15]. However, the mechanical properties of commercially available CPR training manikins remain constant and no information on these properties is not provided. In addition, it is challenging to modify manikins to have various stiffness and damping characteristics. For these reasons, commercially available CPR manikins fail to accurately simulate diverse mechanical behaviors observed in real-life patients. The dissimilarities in mechanical characteristics between manikins and actual patients can result in differences between compression forces and fatigue levels learned from training and those in actual situations. This can impede the delivery of optimal CPR in real-world situations. To provide a CPR training reflecting real-world cases, a manikin that can represent a range of mechanical properties similar to that of a human under compression loadings is needed.

Several studies have proposed manikins that can mimic the non-linear characteristic of human chests [16], [17], [18], [19], [20]. Nysæther et al. [16] have suggested a manikin with a spring and damper inside. The proposed manikin expressed a range of stiffness profiles similar to the measured stiffness of real patients. However, the damping of the manikin was fixed, which limits the range of chest properties it can express. Besides, in order to change the stiffness, the spring must be replaced to other springs with different stiffness profiles.

Stanley et al. [17] have proposed a system with a damper system that is controlled with respect to movement of a manikin's chest to achieve desired amount of damping, taking into account the hysteresis profile of a human chest. The system showed force-displacement curves with hysteresis. However, the constant stiffness and damping characteristics only represent a single instance of human chest properties. Eichhorn et al. [18] have developed a mechanical thorax with adjustable stiffness and mock heart to simulate the blood flow during CPR. The system consisted of springs, pneumatic pistons, one chamber heart and a piston to compress the heart. The stiffness of the system coincides well with that of human chest. Blood flow by compression was also simulated. However, the damping characteristic of the system was not clarified in the study. Kanakapriya and Manivannan [19] and Thielen et al. [20] have suggested systems that include springs connected serially so that stiffness of manikin can increase with increasing compression depth. However, such systems achieved smaller magnitude of stiffness than CPR manikin or human chest.

As far as we know, a manikin that can independently change both stiffness and damping has not been reported yet. When both stiffness and damping are controllable, a CPR manikin has potential to simulate various mechanical properties of human chest and CPR scenarios.

Therefore, the objective of this study was to develop a system with variable stiffness and damping mechanisms for CPR manikin that could simulate mechanical properties similar to human chest and enhance the reality of CPR manikin and CPR training.

II. METHODS

A. DESIGN OF THE SYSTEM

The design of the entire system is shown in Fig. 2(a). Variable stiffness mechanism (VSM) and Variable damper (VD) were devised and implemented to satisfy the range of mechanical characteristics of human chest. Three sets of VSMs and VDs were mounted on a base plate. A pushing plate that could transmit dynamic loading to each set was installed on the top of the VDs. Those mechanisms were implemented for use on a manikin and controlled with a home-made control system to achieve desired mechanical characteristics. All parts were designed using Autodesk Inventor 2023 (Autodesk Inc., US).

1) VARIABLE STIFFNESS MECHANISM (VSM)

As shown in Fig. 2(b), the VSM unit consists of a pair of subassemblies which include spools, servo motors (XH430-V350, Robotis, Korea), and sets of gears and silicone bands that could act like springs. Silicone bands were used to connect the ring-shaped part of cylinders and spools of either side. These silicone bands were manufactured using a silicone material (SH0140U, KCC Co., Korea) with a shore hardness of 40A, a tensile strength of 8.5 MPa, and a maximum elongation rate of 645%. The spools and ring-shaped parts were

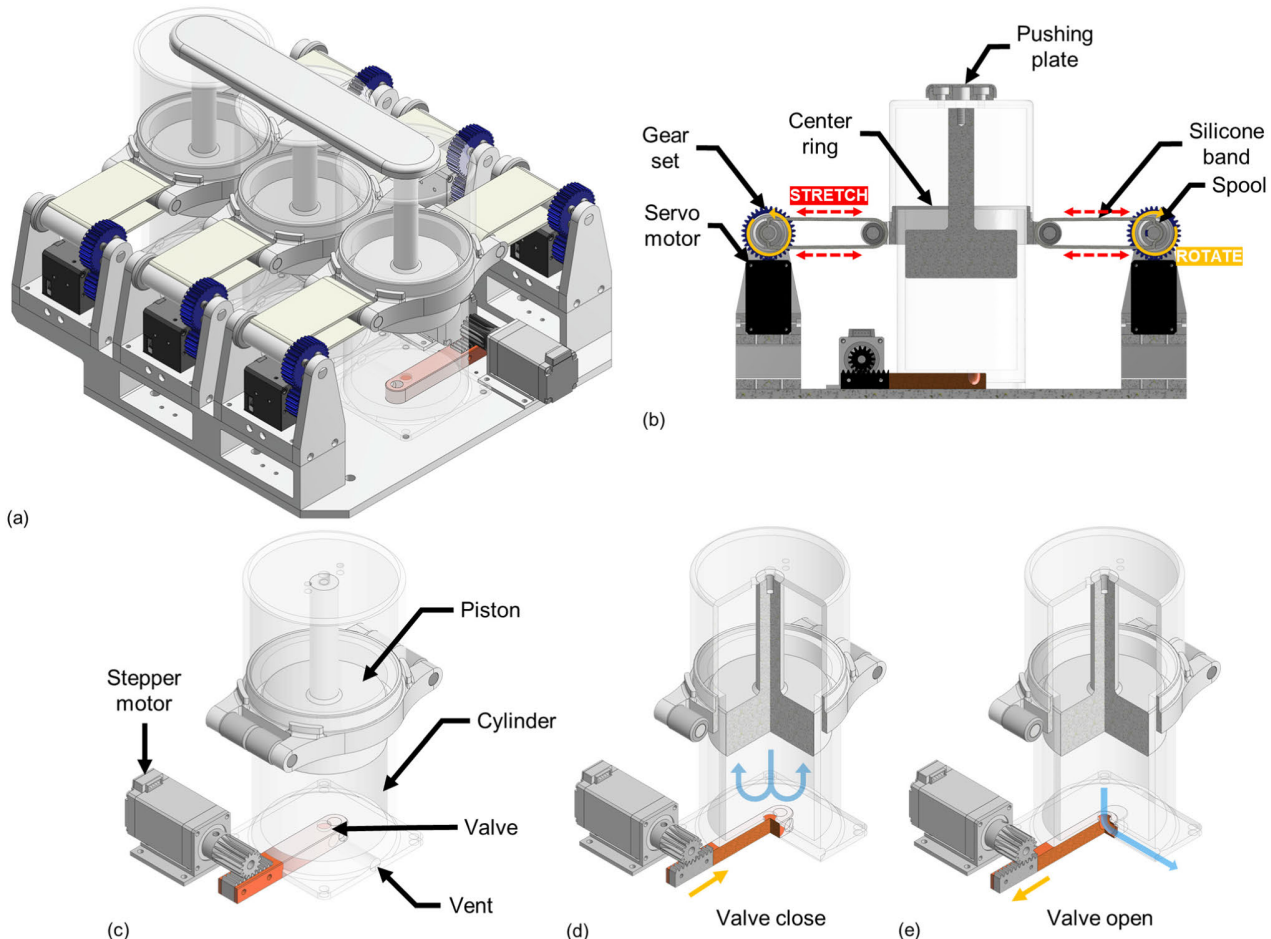


FIGURE 2. Drawings of the variable stiffness mechanism (VSM), the variable damper (VD) and the total system. (a) A total assembly drawing of the system that consists of three sets of VSM and VD. (b) A cross-section view of the VSM unit. As spools rotate, silicone bands are wound or unwound resulting in stiffness modulation. (c) A structure of VD. Controlling the valve beneath the cylinder, damping of the unit is modulated. (d) If the valve is closed when the cylinder stroked, the air (translucent blue arrow) in and around the cylinder can only flow through a small gap between the inner surface of the cylinder and the outer surface of the piston, maximizing the damping. (e) If the valve is open when the cylinder is stroked, most of the air in and around the cylinder can flow through the valve, minimizing the damping.

3D printed (Accura 25 and Projet 7000 HD, 3D Systems Inc., US). The translucent lids were machined from polycarbonate.

When the servo motors were activated, spools rotated outwards (clockwise for right spools, counter clockwise for left spools), causing a portion of the silicone bands to wind on spools. As the bands were wound more, they were stretched further. Thus, required a greater force was required to elongate them. Consequently, the stiffness of the system in response to compression forces was increased.

2) VARIABLE DAMPER (VD)

A dashpot damper with a valve is designed to make damping adjustable as shown in Fig. 2(c).

A piston was inserted into a cylinder that was closed on one side. A hole was placed on the surface of the closed side of the cylinder. A bar with a 90-degree curved circular channel, like an elbow pipe, was placed beneath the cylinder. One end of the channel met the hole of the cylinder while the other

end was directed to a vent. As the piston moved, air flew in and out of the cylinder via this channel (Fig. 2(d) and 2(e)). Linearly translating the bar changes the effective area of the channel cross-section, serving as a valve to modulate the system's damping. The piston was machined from acetal with a diameter of 69.5 mm and a height of 30 mm. The cylinder was made of poly methyl methacrylate (PMMA). The diameters of the hole at the bottom of the cylinder and the channel of the bar are 8 mm. A stepper motor (PKP525N12A, Oriental Motor, Japan) was used for the linear motion of the bar. The maximum stroke of the piston was designed to be 60 mm to satisfy the compression depth requirement of CPR [1].

3) CONTROL SYSTEM

A control system for VSM and VD was built with a Raspberry Pi 4, a servo interface board (U2D2, Robotis, Korea), stepper motor drivers (CVD524BR-K, Oriental Motor, Japan) and a power supply (ADS-15524, Meanwell, US) as depicted in

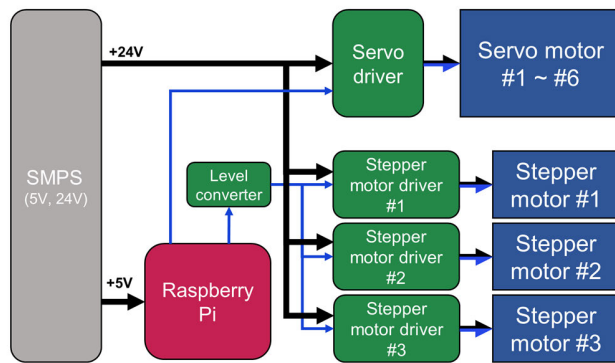


FIGURE 3. Schematic diagram of the control system. Blue line = signal; Black line = power; SMPS: Switching Mode Power Supply.



FIGURE 4. Picture of the experimental setup. Compression loading was achieved with four-degrees-of-freedom(4-DoF) manipulator (U3robotics, Korea).

TABLE 1. Stiffness and damping adjustment range of the system.

Parameter	Value
Spool rotation angle	150 to 480 deg, 30 deg increments
Valve opening rate	0, 10, 20, 30, 40, 60, 80, 100 %

Fig. 3. A program was developed on Raspberry Pi to control rotation amounts of each spool and aperture opening areas of each damper.

B. PERFORMANCE TEST

1) COMPRESSION TESTS WITH PARAMETERS ADJUSTMENT

Compression tests were conducted to validate mechanical behavior of the system according to the setup shown in Fig. 4.

As shown in Table 1, 12 rotation angles for the spools and eight opening rates of the apertures were decided. A combination of these gave 96 cases to evaluate.

From the smallest stiffness condition to the largest stiffness condition, 30 compressions were performed serially at a rate of 100 compressions per minute with a depth of 5 cm using a four-degree-of-freedom(4-DoF) manipulator (U3robotics, Korea). A preload was applied at around 20 N of magnitude before starting each test to ensure contact between the manipulator and the system.

To avoid any changes in mechanical properties of the silicone bands across the entire stress range from minimum to maximum, tests were repeated in the same order after all tests had been completed.

Compression force and depth were collected at a rate of 1000 Hz from sensors embedded in the robot manipulator.

2) MECHANICAL CHARACTERISTIC ANALYSIS

From collected force and displacement data, spring constant and damping coefficient were calculated. With methods described in [21], stiffness k and damping coefficient c were analyzed.

From the equation of motion of the system, external force F_{ext} can be written as follows:

$$F_{ext} = kd + cd = kd + cv \quad (1)$$

where d is the displacement and v is the speed of manipulator differentiated from the depth by time. Equation (1) can be rewritten to show compression period and releasing period as follows:

$$F_{comp} - kd_{comp} - cv_{comp} = F_{release} - kd_{release} - cv_{release} \quad (2)$$

Since the difference between the force required for compression and the force used for recoil comes from the change in damping at each period, equation (2) can be written as follows:

$$F_{comp}(d) - F_{release}(d) = c(d)(v_{comp} - v_{release}) \quad (3)$$

Rearranging Equation (3), $c(d)$ can be obtained as follows:

$$c(d) = \frac{F_{comp}(d) - F_{release}(d)}{v_{comp}(d) - v_{release}(d)} \quad (4)$$

Rewriting equation (1) with respect to k , $k(d)$ can be derived as follows:

$$k(d) = \frac{F_{comp}(d) - c(d)v_{comp}(d)}{d_{comp}} \quad (5)$$

Values for $k(d)$ and $c(d)$ were computed from these equations using MATLAB R2023b (Mathworks, US) for each case. These values were then compared with stiffness and damping values suggested in previous study [14].

3) STABILITY TEST

A long-term cyclic loading experiment was conducted to assess the reproducibility of the silicone bands that represent system's stiffness under repeated loading.

A set of one VSM and one VD was constructed and assembled for this experiment. A pair of unused silicone bands were

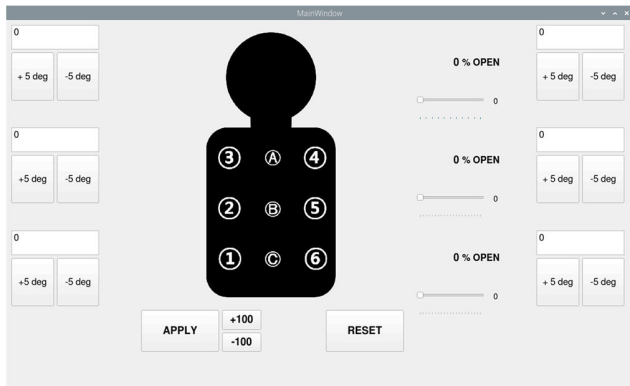


FIGURE 5. Screenshot of control program of the system. Numbers 1 to 6 represent servo motors. A, B, and C represent stepper motors.

installed in the VSM. The same robot manipulator used in the previous performance test was also used for this test.

The stiffness was set to the maximum rotation angle of 480 degrees. The damper valve was opened to 100 %. This setting could provide a maximum reaction force of approximately 240 N. Since the original system consisted of three sets of VSM and VD, this test setting corresponded to the maximum reaction force of 720 N, surpassing the force in the range of 300 to 600 N typically required for actual CPR [21]. Compression conditions were set to be the same as those for the performance test (depth of 5 cm, compression rate of 100 compressions/min).

Repetitive compression was conducted for 90 minutes, resulting in approximately 90,000 cycles. After compression, magnitudes of the initial and final peak reaction forces were compared, followed by the analysis of variation in reaction forces during the test.

III. RESULTS

A. DESIGN OF THE SYSTEM

The system was built as shown in Fig. 6(a). Its dimension was $280.5 \times 297 \times 196.3$ mm. It could be installed in a modified Little Anne (Laerdal Medical, Norway) CPR training manikin (Fig. 6(b)) by removing the inner center post for the spring to be inserted.

A control system and program for motor control was made. The servo motors utilized for stiffness control were programmed to rotate in increments of five degrees and they were controlled with a devised program as shown in Fig. 5. Stepper motors for damping were programmed to regulate the rate of cross-sectional area of the airway in 10% increments.

B. PERFORMANCE TEST

1) COMPRESSION TEST

Figs. 7(a) and 7(b) show force-displacement curves of varying damping with fixed stiffness conditions. As the rate of opening area of valves increased (damping decreases), the area between compression and release curves became smaller. However, the mean slope of the curves remained

almost constant. This means that energy dissipation due to damping is well implemented in the system.

A result of varying the stiffness with a fixed damping condition is shown in Fig. 7(c). Since the damping was constant, areas between the compression and recoil curves remained constant while the slope of curves increased with stiffness.

These results show that the system can simulate a range of non-linear mechanical characteristics by regulating damping and stiffness independently.

2) MECHANICAL CHARACTERISTIC ANALYSIS

Stiffness and damping coefficients according to compression depth calculated from compression test data set (88 cases) are presented in Figs. 7(d) and 7(e).

The damping exhibited a nonlinear characteristic along the compression depth. This characteristic was believed to be due to the compression waveform. Given that the compression waveform was trapezoidal, the velocity of compression at the depths below 1 cm, and over 4 cm changed rapidly. It was assumed that the damping of the system was adequately presented in the constant velocity region between 1 and 4 cm. Therefore, damping values within the depth range of 1 to 4 cm were determined and plotted.

The value of damping at 30 mm depth ranged from 0.127 N·s/m to 0.511 N·s/m. The value of stiffness at maximum depth ranged from 5.34 to 13.59 N/mm. As reported in previous study [16], the stiffness at a depth of 50mm and the damping at a depth of 30 mm was between 4 N/mm and 10 N/mm, and 0.08 N·s/mm and 0.38 N·s/mm for patients. Our system was able to represent most of these ranges of stiffness and damping for patients, with the exception of the lowest bound where the system can express greater values of stiffness and damping than these ranges.

3) STABILITY TEST

As shown in Fig. 7(f), the reaction force decreased as the cyclic load was maintained for about 90 minutes. The final number of cycles was 8884. From the initial to the 10th cycle, the cycle-to-cycle force reduction was greater than 0.5 N and the force decreased from 285 N to 250 N. The magnitude of reduction subsequently decreased, reaching less than 0.01 N from approximately the 500th cycle. This value was notably small. Therefore, the 500th cycle was set as the point at which the force started to stabilize. From that point to the last cycle, the reaction force decreased from 248 N to 235 N, presenting a 5 % reduction.

IV. DISCUSSION

The human chest can be represented by mechanical properties such as stiffness and damping, which can vary with age, gender, and body weight. However, limited mechanical properties of commercial manikins might not be able to represent realistic human chest characteristics for CPR training or research. Therefore, a system for CPR manikin

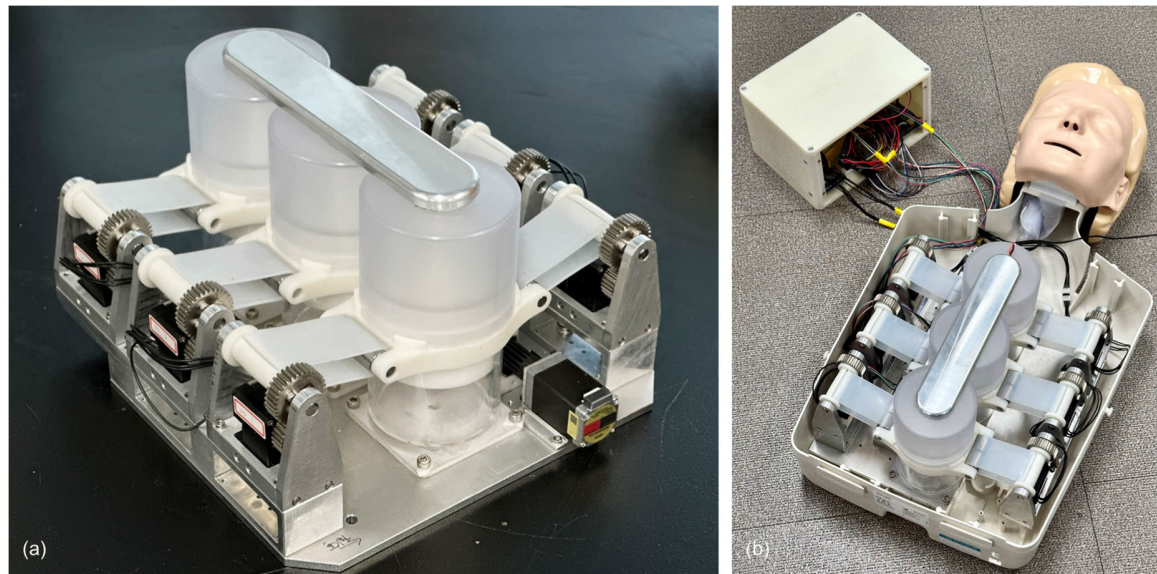


FIGURE 6. (a) The complete system as built. (b) The system installed in Little Anne(Laerdal Medical, Norway) CPR manikin.

to simulate non-linear characteristic of a real human chest was constructed. The proposed system can obtain various mechanical characteristics by modulating the stiffness and damping independently. The stiffness of the system can be controlled in the range of measured human chest stiffness by pre-stretching silicone bands. This approach represents a new method for controlling stiffness that differs from the use of springs in previous studies. Additionally, the system utilized controllable dashpot dampers with valves that could allow the system to express various damping characteristics to include those of human chests presented in several studies [13], [16], [21]. Various mechanical characteristics can be achieved to mimic the human chests by modulating the stiffness and damping independently. A stability test was conducted to determine whether the stiffness of the newly proposed band-based stiffness control system remained the same during repetitive compressions. Results revealed that, the system showed enough stability even after 8,000 cyclic loads. Damping of the system was largely determined by the opening area of the valve. Therefore, damping was rarely changed over the prolonged compressions. The initial rapid change of stiffness was likely due to Mullin's effect, a phenomenon where an initial stress is applied to an elastic material and then less stress is appeared for the same strain [22]. After approximately 8,000 cycles, the reaction force underwent a change of only 0.1% over subsequent cycles. This relatively minor alteration was difficult to discern. Therefore, the stiffness and damping will be nearly identical for each user after the completion of 8,000 cycles of pre-compression.

The system has some advantages over commercial manikins and previous studies on CPR manikin. First, the system can represent various non-linear characteristic of a human chest and hysteresis resulting from damping without replacing any parts. Desired mechanical property can

be achieved only by controlling motors of the system with control software.

Secondly, it is the only system that can control both damping and stiffness independently so far. The system can simulate numerous cases by combining the damping and the stiffness parameters while the others can mimic few cases by changing only stiffness or damping.

These advantages can improve CPR training by providing trainee with experience of chest compression similar to real human chest and widening scenarios of training with a variety of chest properties. Besides for training, this system can be used for validating performances of CPR devices currently under development, owing to its capability to simulate diverse mechanical properties of the chest. Additionally, this system holds promise for facilitating research aimed at determining the optimal compression force and depth of CPR across varying mechanical profiles of patients.

The system also has some limitations. First, the complexity and the weight of the system may reduce its usability. Since the system includes six servo motors and three stepper motors, many wires and peripherals are needed to actuate all motors. Also, most parts of the system are made of aluminum to ensure stability. As a result, the system weighs around 8 kg, much heavier than commercial manikins. Also, the system can be simpler if dedicated control board is used instead of raspberry pi or motor drivers used for universal usage. In addition, optimizing the structural design and materials can lead to lighter system to be carried easily.

Although our proposed system has limitations in weight and complexity, it has the advantage of being a system that can simulate mechanical properties of the human chest by adjusting various stiffness and damping that can advance CPR training and research. For future studies, we plan to develop a new control program to simulate various situations such as a

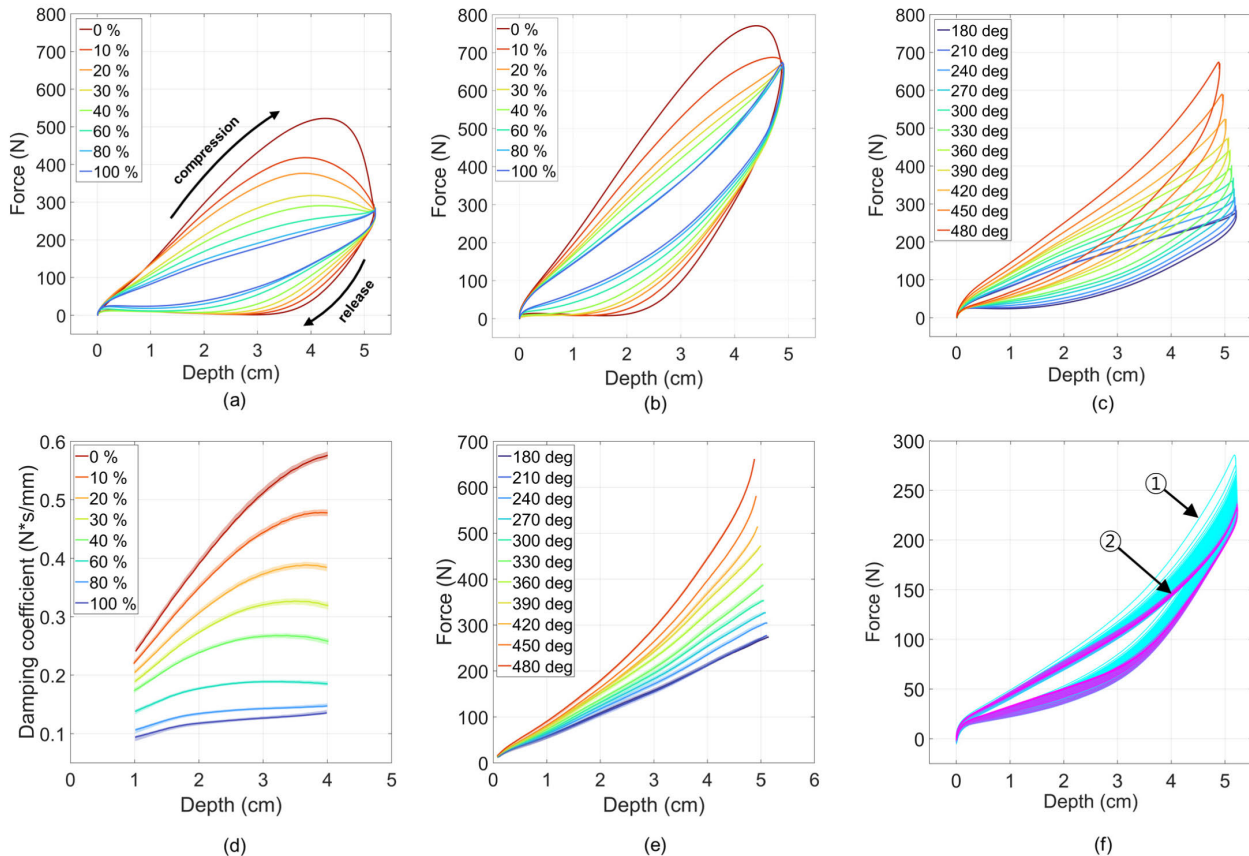


FIGURE 7. Results of performance tests and mechanical characteristic analysis. (a) Force-displacement curves of the minimum stiffness condition (180 degrees of spool rotation) with varying damping. As damping increases (valve opening rate goes to 0), the area between compression and release curves becomes larger, which means that energy dissipation due to damping increases. (b) Force-displacement curves of the maximum stiffness condition (480 degrees of spool rotation) with varying damping. Similar to (a), the area between compression and release curves becomes larger as damping increases, which means that the energy dissipation due to damping increases. (c) Force-displacement curves of the minimum damping condition (valve fully open) with varying stiffness. The slope of each stiffness case increases as the stiffness increases, while the area between the compression and release curves remains almost constant. (d) Damping characteristics of the system. The amount of the damping increases as the valve opening rate decreases, depending on the compression depth at the same time. (e) Stiffness characteristics of the system. The stiffness increases as the spool rotation angle and compression depth increase. (f) Force - displacement curves of the entire cyclic loadings during stability test. ① is the first cycle, and ② is the last cycle. Although the stiffness and hysteresis of the system decreased as the loading repeated, from the 500th cycle to the last (8884th) cycle, the reaction force only decreased 5 %.

slanted angle of sternum in real human thorax and dislocation or fracture of cartilage and rib during CPR. Additionally, a qualitative study will be conducted with experts, including clinicians, to evaluate how well the system can mimic the real human chest.

V. CONCLUSION

We constructed a new system for CPR manikin to simulate mechanical properties of human chests using adjustable damping and stiffness mechanisms. The system shows non-linear mechanical characteristics due to viscous damping like human chest under compression loadings. Such characteristics could be adjusted by controlling both stiffness and damping. The system is capable of simulating a wide range of stiffness and damping in the human chest. It has the potential to be utilized in various CPR training and research for more realistic results.

REFERENCES

- [1] A. R. Panchal et al., “Part 3: Adult basic and advanced life support: 2020 American heart association guidelines for cardiopulmonary resuscitation and emergency cardiovascular care,” *Circulation*, vol. 142, no. 2, pp. S366–S468, Oct. 2020, doi: [10.1161/cir.0000000000000916](https://doi.org/10.1161/cir.0000000000000916).
- [2] K. B. Kern, R. W. Hilwig, R. A. Berg, A. B. Sanders, and G. A. Ewy, “Importance of continuous chest compressions during cardiopulmonary resuscitation,” *Circulation*, vol. 105, no. 5, pp. 645–649, Feb. 2002, doi: [10.1161/hc0502.102963](https://doi.org/10.1161/hc0502.102963).
- [3] J. Christenson et al., “Chest compression fraction determines survival in patients with out-of-hospital ventricular fibrillation,” *Circulation*, vol. 120, no. 13, pp. 1241–1247, Sep. 2009, doi: [10.1161/circulationaha.109.852202](https://doi.org/10.1161/circulationaha.109.852202).
- [4] A. H. Idris et al., “Chest compression rates and survival following out-of-hospital cardiac arrest,” *Crit. Care Med.*, vol. 43, no. 4, pp. 840–848, Apr. 2015, doi: [10.1097/ccm.0000000000000824](https://doi.org/10.1097/ccm.0000000000000824).
- [5] T. Vadéboncoeur et al., “Chest compression depth and survival in out-of-hospital cardiac arrest,” *Resuscitation*, vol. 85, no. 2, pp. 182–188, Feb. 2014, doi: [10.1016/j.resuscitation.2013.10.002](https://doi.org/10.1016/j.resuscitation.2013.10.002).
- [6] S. Duval et al., “Optimal combination of compression rate and depth during cardiopulmonary resuscitation for functionally favorable survival,” *JAMA Cardiol.*, vol. 4, no. 9, p. 900, Sep. 2019, doi: [10.1001/jamacardio.2019.2717](https://doi.org/10.1001/jamacardio.2019.2717).

- [7] I. N. Bankman, K. G. Gruben, H. R. Halperin, A. S. Popel, A. D. Guerci, and J. E. Tsitlik, "Identification of dynamic mechanical parameters of the human chest during manual cardiopulmonary resuscitation," *IEEE Trans. Biomed. Eng.*, vol. 37, no. 2, pp. 211–217, 1990, doi: [10.1109/10.46262](https://doi.org/10.1109/10.46262).
- [8] B. K. Arbogast, R. M. Maltese, M. V. Nadkarni, A. P. Steen, and B. J. Nysaether, "Anterior-posterior thoracic force-deflection characteristics measured during cardiopulmonary resuscitation: Comparison to post-mortem human subject data," *Stapp Car Crash J.*, vol. 50, pp. 131–145, Nov. 2006.
- [9] S. M. Kang and S. W. Choi, "Monitoring mechanical impedance of the thorax with compression and decompression cardiopulmonary resuscitation device," *J. Mech. Sci. Technol.*, vol. 33, no. 2, pp. 981–988, Feb. 2019, doi: [10.1007/s12206-019-0155-y](https://doi.org/10.1007/s12206-019-0155-y).
- [10] J. M. Dean et al., "Age-related changes in chest geometry during cardiopulmonary resuscitation," *J. Appl. Physiol.*, vol. 62, no. 6, pp. 2212–2219, Jun. 1987, doi: [10.1152/jappl.1987.62.6.2212](https://doi.org/10.1152/jappl.1987.62.6.2212).
- [11] H.-Y. Choi and D.-S. Kwak, "Morphologic characteristics of Korean elderly rib," *J. Automot. Saf. Energy*, vol. 2, no. 2, p. 122, 2011.
- [12] C. Pezowicz and M. Glowacki, "The mechanical properties of human ribs in young adult," *Acta Bioeng. Biomech.*, vol. 14, no. 2, pp. 53–60, 2012, doi: [10.5277/abb120207](https://doi.org/10.5277/abb120207).
- [13] S. Ruiz de Gauna et al., "Characterization of mechanical properties of adult chests during pre-hospital manual chest compressions through a simple viscoelastic model," *Comput. Methods Programs Biomed.*, vol. 242, Dec. 2023, Art. no. 107847, doi: [10.1016/j.cmpb.2023.107847](https://doi.org/10.1016/j.cmpb.2023.107847).
- [14] S. Beger et al., "Chest compression release velocity factors during out-of-hospital cardiac resuscitation," *Resuscitation*, vol. 145, pp. 37–42, Dec. 2019, doi: [10.1016/j.resuscitation.2019.09.024](https://doi.org/10.1016/j.resuscitation.2019.09.024).
- [15] J. K. Russell, M. Leturiondo, D. M. González-Otero, J. J. Gutiérrez, M. R. Daya, and S. R. de Gauna, "Chest compression release and recoil dynamics in prolonged manual cardiopulmonary resuscitation," *Resuscitation*, vol. 167, pp. 180–187, Oct. 2021, doi: [10.1016/j.resuscitation.2021.08.036](https://doi.org/10.1016/j.resuscitation.2021.08.036).
- [16] J. B. Nysaether, E. Dorph, I. Rafoss, and P. A. Steen, "Manikins with human-like chest properties—A new tool for chest compression research," *IEEE Trans. Biomed. Eng.*, vol. 55, no. 11, pp. 2643–2650, Nov. 2008, doi: [10.1109/TBME.2008.2001289](https://doi.org/10.1109/TBME.2008.2001289).
- [17] A. A. Stanley, S. K. Healey, M. R. Maltese, and K. J. Kuchenbecker, "Recreating the feel of the human chest in a CPR manikin via programmable pneumatic damping," in *Proc. IEEE Haptics Symp. (HAPTICS)*, Mar. 2012, pp. 37–44, doi: [10.1109/HAPTIC.2012.6183767](https://doi.org/10.1109/HAPTIC.2012.6183767).
- [18] S. Eichhorn et al., "Development and validation of an improved mechanical thorax for simulating cardiopulmonary resuscitation with adjustable chest stiffness and simulated blood flow," *Med. Eng. Phys.*, vol. 43, pp. 64–70, May 2017, doi: [10.1016/j.medengphy.2017.02.005](https://doi.org/10.1016/j.medengphy.2017.02.005).
- [19] K. Kanakapriya and M. Manivannan, "CPR module with variable chest stiffness in high fidelity mannequins," in *Proc. CIRP Design*, 2013, pp. 159–167, doi: [10.1007/978-1-4471-4507-3_16](https://doi.org/10.1007/978-1-4471-4507-3_16).
- [20] M. Thielen, R. Joshi, F. Delbressine, S. Bambang Oetomo, and L. Feijis, "An innovative design for cardiopulmonary resuscitation manikins based on a human-like thorax and embedded flow sensors," *Proc. Inst. Mech. Eng., H. J. Eng. Med.*, vol. 231, no. 3, pp. 243–249, Mar. 2017, doi: [10.1177/0954411917691555](https://doi.org/10.1177/0954411917691555).
- [21] A. Neurauter et al., "Comparison of mechanical characteristics of the human and porcine chest during cardiopulmonary resuscitation," *Resuscitation*, vol. 80, no. 4, pp. 463–469, Apr. 2009, doi: [10.1016/j.resuscitation.2008.12.014](https://doi.org/10.1016/j.resuscitation.2008.12.014).
- [22] J. Diani, B. Fayolle, and P. Gilormini, "A review on the mullins effect," *Eur. Polym. J.*, vol. 45, no. 3, pp. 601–612, Mar. 2009, doi: [10.1016/j.eurpolymj.2008.11.017](https://doi.org/10.1016/j.eurpolymj.2008.11.017).

• • •